Steel and Composite Structures, *Vol. 19, No. 6 (2015) 1531-1548*
DOI: http://dx.doi.org/10.12989/scs.2015.19.6.1531

Relationship between Barcol hardness and flexural modulus degradation of composite sheets subjected to flexural fatigue

Raif Sakin*

Department of Machine and Metal Technologies, Edremit Vocational School of Higher Education, Balıkesir University, 10300, Edremit, Balıkesir, Turkey

(*Received September 22, 2014, Revised April 24, 2015, Accepted July 11, 2015*)

Abstract. The aim of this study is to investigate the relationship between Barcol hardness (H) and flexural modulus (E) degradation of composite sheets subjected to flexural fatigue. The resin transfer molding (RTM) method was used to produce 3-mm-thick composite sheets with fiber volume fraction of 44%. The composite sheets were subjected to flexural fatigue tests and Barcol scale hardness measurements. After these tests, the stiffness and hardness degradations were investigated in the composite sheets that failed after around one million cycles (stage III). Flexural modulus degradation values were in the range of 0.41-0.42 with the corresponding measured hardness degradation values in the range of 0.25-0.32 for the all fatigued composite sheets. Thus, a 25% reduction in the initial hardness and a 41% reduction in the initial flexural modulus can be taken as the failure criteria. The results showed that a reasonably well-defined relationship between Barcol hardness and flexural modulus degradation in the distance range.

Keywords: glass-fiber; fatigue; hardness (H) and flexural modulus (E); degradation; hardness-stiffness relationship

1. Introduction

The elastic modulus (*E*) and the hardness (*H*) are two essential parameters describing the behavior of structural materials, and the relationship between them is of keen interest to material scientists. From a statistical standpoint, *E* is an increasing function of *H*, but this rule has neither analytical support nor is it generally obeyed (Bao *et al*. 2004). The *E*/*H* ratio is useful in describing the deformation of materials. The modulus is the material's resistance to elastic deformation, and the hardness is the material's resistance to local plastic deformation (Xu *et al*. 2000). The relationship between Shore and ISO hardness and Young's modulus was investigated in detail by Gent, who derived a semi-empirical equation (Meththananda *et al*. 2009).

The recent advent of glass-fiber-reinforced plastics (GFRPs) as a popular construction material in aerospace, marine, wind turbine, land transportation, and automotive industries underscores the need for reliable fatigue-life prediction methodologies for this important class of advanced materials. A good fatigue-life prediction model should consider the real fatigue damage processes operative during the cyclic loading, so that it can be employed to provide reliable and sound fatigue-life predictions that can be used, with a reasonable confidence, in design, service, and

*Corresponding author, Ph.D., E-mail: rsakin@balikesir.edu.tr

http://www.techno-press.org/?journal=scs&subpage=8 ISSN: 1229-9367 (Print), 1598-6233 (Online)

maintenance of engineering components and structures made of fiber reinforced plastics (Khan *et al*. 2001). During the last two decades, a number of theoretical and empirical models based on the fatigue damage mechanics, damage mechanisms, and the observed effects of fatigue damage on the strength or the stiffness of various fiber reinforced plastics have been proposed (Khan *et al*. 2001). There are a few studies in the literature that investigate the relationship between H and E in fatigued composites. Philippidis and Vassilopoulos (1999) have shown that the change in E depends on the off-axis loading as much as on the applied cyclic stress level. Poursartip and Beaumont (1983) have shown that in carbon-fiber composite laminates failure occurs when the stiffness of the material $E = 0.65E_0$, where E_0 is the stiffness of the material before loading (Natarajan 2005). Bezazi *et al*. (2007) obtained data showing stiffness degradation of sandwich composites against the number of fatigue cycles. In this study, the stiffness degradation was defined in terms of load (i.e., F/F_0).

It is commonly accepted that for the vast majority of fiber-reinforced composite materials, the deterioration in the modulus can be divided into three stages: the initial decrease, an approximately linear reduction, and final failure, as shown in Fig. 1(a).

- The initial region (”stage I”) features a rapid stiffness reduction of 2–5%. The development of transverse matrix cracks dominates the stiffness reduction in this first stage (Paepegem and Degrieck 2002). As reported by Vavouliotis *et al*. (2011) and illustrated in Fig.1(b), the initial region of damage development is associated with multiple matrix cracks forming along fibers in off-axis plies, culminating in a saturation of cracks in individual plies. This generic pattern of matrix cracking is termed the “characteristic damage state” (CDS), and is a characteristic of the lay-up of the material.
- An intermediate region (“stage II”), in which an additional 1–5% stiffness reduction occurs in an approximately linear fashion with respect to the number of cycles. Predominant damage mechanisms are edge delamination and additional longitudinal cracks developing along the 0° fibers (Paepegem and Degrieck 2002). In this state following the CDS, the ply cracks link up locally by debonding the ply-to-ply interface. Further loading cycling causes the growth and coalescence of delaminated regions (Vavouliotis *et al*. 2011).

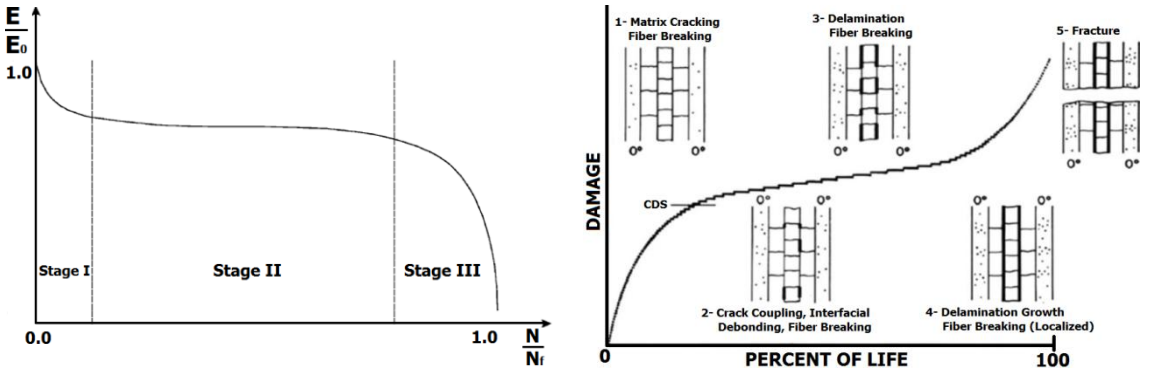

(a) Typical stiffness degradation curve for a wide range of fiber-reinforced composite materials (Paepegem and Degrieck 2002)

(b) The stages of damage development over the fatigue lifetime of a composite material (Vavouliotis *et al*. 2011)

Fig. 1 Degradation of fiber composites under fatigue loading

- A final region ("stage III"), in which stiffness reduction occurs in abrupt steps ending in specimen fracture. In stage III, a transfer to local damage progression occurs, corresponding to when the initial fiber fractures develop into strand failures (Paepegem and Degrieck 2002). In other words, the damage process is characterized by fiber breakage in the longitudinal plies and total failure (Vavouliotis *et al*. 2011).

The damage variable (D) is a measure of stiffness degradation (Paepegem and Degrieck 2002, Kumar *et al*. 2007) and is given by

$$D = 1 - (E/E_0). \tag{1}$$

Studies regarding stiffness degradation in hybrid glass–carbon fiber reinforced epoxy matrix composites were performed by Belingardi and Cavatorta (2006). Displacement-controlled bending fatigue tests with an R ratio of 0.10 were conducted on standard specimens, and damage in the composite was continuously monitored through the loss of bending moment during cycling (Belingardi and Cavatorta 2006, Belingardi *et al*. 2006).

In the study have done by Selmy *et al*. (2013), the cantilever-type flexural fatigue tests were conducted on unidirectional glass fiber/epoxy composite laminates. The reciprocating arm of the testing machine was used to measure the residual flexural stiffness ratio $EI/(EI)_0$ by setting the amplitude of the reciprocating arm to be a linear function of the applied bending moment on the test specimen. The test specimen deflection (δ) is given by

$$\delta = \frac{P\,L^3}{3\,E\,I} \tag{2}$$

where P is the applied load on the test specimen and L is the cantilever length of the test specimen.

The study conducted by Allah *et al*. shows the relationship between $EI/(EI)_0$ and the cycle ratio N/N_f, where N_f is the number of cycles to failure. The results illustrate that the stiffness of the test specimens decreased by 25% at a cycle ratio $N/N_f \approx 0.04$. The initial, rapid stiffness reduction was followed by a slow one, linear reduction until the test was halted after a 30% drop in specimen stiffness was obtained (Abd-Allah *et al*. 1997).

To further summarize the literature, the following parameters have been used variously as failure criteria to describe the stiffness degradation in the composite material during fatigue testing

- the loss of applied load (Philippidis and Vassilopoulos 1999, Paepegem and Degrieck 2002, El Mahi *et al*. 2004, Bezazi *et al*. 2007)
- the loss of applied stress (Poursartip and Beaumont 1983)
- the loss of max. strain rate (Natarajan 2005, Kensche 2006)
- the loss of max. displacement (El Mahi *et al*. 2004)
- the loss of static strength (Mayer 1996)
- the loss of bending moment (Belingardi and Cavatorta 2006, Belingardi *et al*. 2006, Koricho *et al*. 2014)
- the loss of flexural strength (Kar *et al*. 2011)
- the loss in strain energy per cycle (Natarajan 2005)
- the electrical resistance change (Vavouliotis *et al*. 2011)
- the loss of EI (Abd-Allah *et al*. 1997, Kar *et al*. 2011, Selmy *et al*. 2013)

In the current study, the failure criteria are defined as the degradations of the Barcol hardness

and the flexural modulus.

2. Materials and methods

2.1 GFRP materials

E-glass woven-roving with four different weights and chopped strand-mat with two different weights were mixed with polyester resin to fabricate composite sheets by the resin transfer molding (RTM) method. In order to obtain the GFRP sample by the RTM method a heated mold

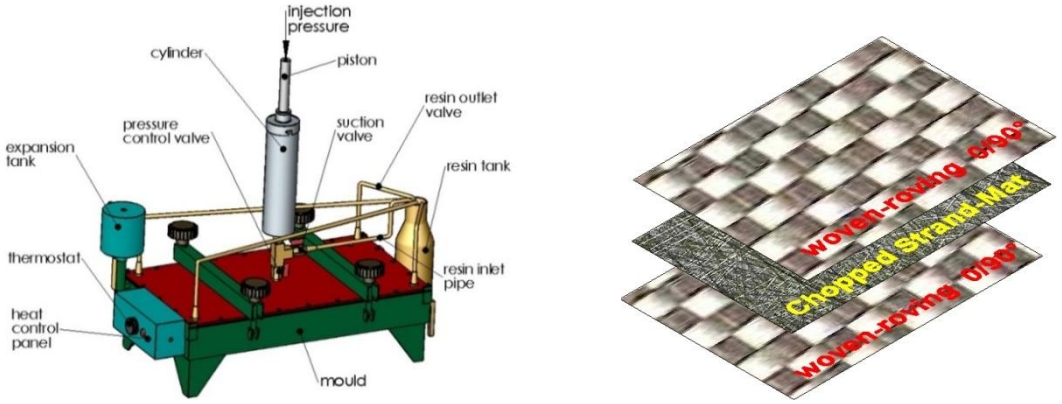

(a) (b)

Fig. 2 (a) application and schematic picture of RTM method; and (b) placement of glass fibers

Table 1 Components of the GFRP sheets and their properties

Matrix	Orthophthalic polyester resin [a] Polipol™ 351, ρ = 1.128 g/cm^3 Barcol Hardness = 44 (Barcol 934-1) Flexural Strength = 140 MPa Flexural *E*-Modulus = 4093 MPa Tensile Strength = 66 MPa Tensile *E*-Modulus = 3234 MPa Poisson's Ratio = 0.36 Elongation at break = 4.1%	**Reinforcement**	E-glass woven-roving [b,c] ρ =2.54 g/cm^3 Weights = 800-500-300-200 g/m^2 E-glass chopped strand-mat [b,c] ρ = 2.54 g/cm^3 Weights = 225-450 g/m^2 Typical diameter = 12-17 μm Tensile strength = 2306 MPa Tensile *E*-modulus = 72.4-81.5 GPa Poisson's ratio = 0.22 Ultimate elongation = 2.97%
Monomer	Styrene [a], ρ = 0.906 g/cm^3		
Hardener	MEKP [a] (Methyl Ethyl Ketone Peroxide) (0.7% of matrix volume)	**Mixing matrix**	Polyester (85%) + Styrene (15%) ρ = 1.095 g/cm^3
Catalyst	Cobalt Naphthenate[a] (0.2% of matrix volume)	**GFRP sheets**	ρ = 1.73 g/cm^3

[a] Poliya A.Ş.; [b] Cam Elyaf A.Ş.; [c] Fibroteks A.Ş. (in Turkey)

Table 2 GFRP sample groups, their defining parameters, and the number of layers in each (V_f = 44%)

Samples groups	E-glass woven-roving				E-glass chopped strand-mat	
	Weight per unit area (g/m^2)					
	800	500	300	200	225	450
#800	3[d]	-	-	-	4	-
#500	-	4	-	-	4	1
#300	-	-	5	-	4	2
#200	-	-	-	7	8	-

[d] Indicates the number of fabric layers in the sample

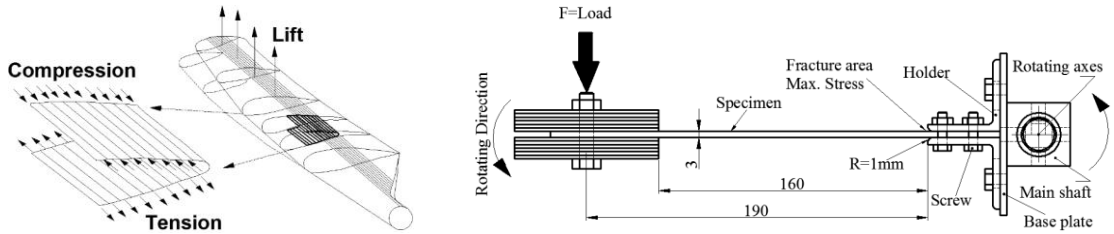

(a) (b)

Fig. 3 Turbine blade service conditions and composite fatigue testing: (a) Representation of the lift force on a wind turbine blade; and (b) a simplified fatigue test geometry

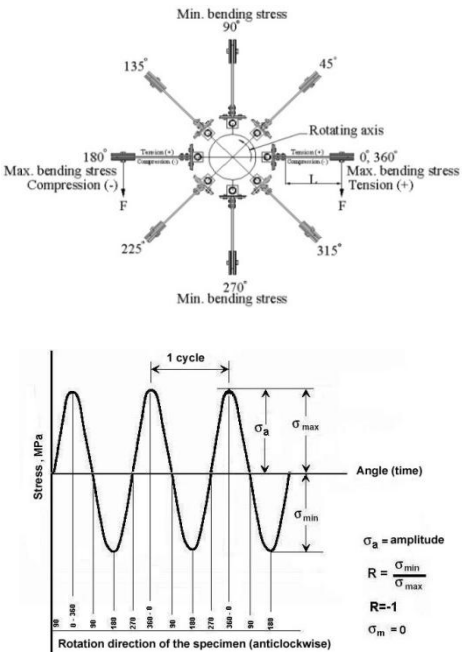

Fig. 4 Stresses in the rotating specimen. Snapshots of the end-weighted specimen rotating about the central shaft; sinusoidal bending stresses result

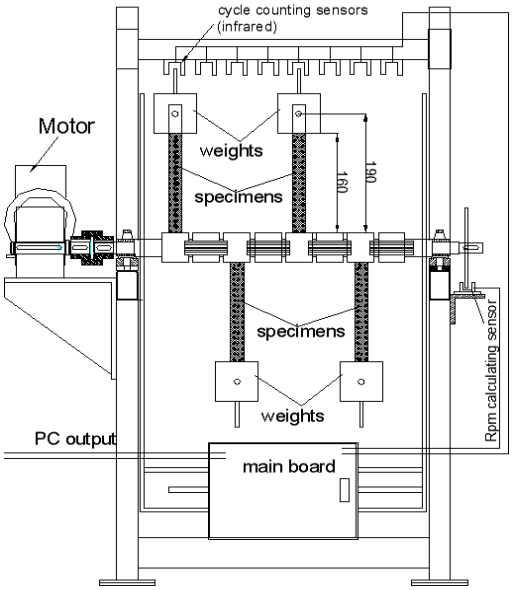

Cantilever plane-bending fatigue
(16 specimens at a time)

Fig. 5 The multi-specimen test setup. The test device for glass / polyester composite specimen fatigue testing can accommodate up to four specimens at once

Table 3 The parameters of the fatigue test

Test parameters	In the current study	In large-scale wind turbine blades
Loading control	Load-controlled	Load-controlled
Fatigue type	Cantilever plane-bending	Cantilever plane-bending
Load source	Metal weights	Wind lift force
Maximum frequency	30 rpm (0.5 Hz)	15-30 rpm
Loading rate	R = -1 (fully-reversed)	R = -1 (fully-reversed)
Motor / Power	0.5 HP - 1390 rpm	1-3 MW
Temperature	Room temperature	Ambient temperature
The number of tested sample	5 (for each stress level)	
Total samples (tested)	140	
Number of cycle	1 million	

2.2 Fatigue testing and modeling

Large-scale wind turbine blades (blade length: 25-50 m, power: 1-3 MW) typically turn at speeds of 15-30 rpm (Jha 2012). Wind forces have a relatively low frequency, a high amplitude, and are the dominant forces driving fatigue in turbine blades (Goeij *et al*. 1999). The airflow generates a lift force causing a bending moment in the blades. In the simplified representation of Fig. 3, the upper side of the blade is under compression, and the lower side under tension. The sinusoidal bending stress (or equivalent imposed deformation) in a lift-generating composite surface is illustrated in Fig.4. A bending moment imposed on the surface by lifting loads will only produce bending stresses in the blade (Goeij *et al*. 1999). This geometry also generates alternating bending stresses, causing fatigue damage over time (Ay *et al*. 2008). Kumar *et al*. determined the degradation in the turbine blade stiffness by changing in rotating frequency as low-cycle fatigue damage. A finite-element approach was used to simulate the evolution of low cycle fatigue damage in the turbine blade. The turbine blade was modeled as a rotating Timoshenko beam with taper and twist. The obtained numerical results were used to investigate the effect of damage growth on the rotation frequencies. It was found that low cycle fatigue was caused sufficient degradation in the blade stiffness by changing the rotating frequency (Kumar *et al*. 2007).

The *S-N* curves and exponential fits from a regression analysis of the GFRP samples are shown in Fig. 6. A power function was used to fit fatigue test data (Ay *et al*. 2008, Sakin and Ay 2008, Sakin *et al*. 2008, Selmy *et al*. 2013)

$$S_f = m \,.\, (N_f)^n \tag{3}$$

where S_f is the stress amplitude, N_f is the mean fatigue life, m is the constant, and n is the power-law exponent. Thus, the fatigue strengths (endurance limits) at one million cycles were obtained from Eq. (3). In addition, standard tensile (ASTM-D3039/D3039M 2008) and three-point bending tests (ASTM-D7264/D7264M 2007, ASTM-D790 2010) were performed. Thus, the tensile and flexural properties of the GFRP samples were determined. The tensile, flexural and fatigue strengths are given in Table 4. The relationships among the hardness, the flexural strength, and the flexural modulus of unfatigued composite specimens are presented in Table 5. The photographs of unfatigued (original) and fatigued composite sheets that failed after one million cycles were shown in Fig. 7.

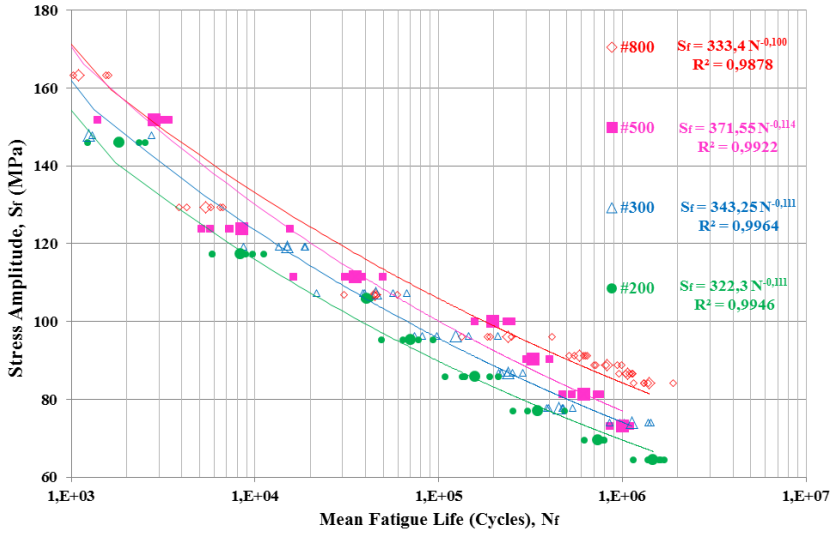

Fig. 6 *S-N* curves for all sample groups. The fits to a power-law function $S_f = m.(N_f)^n$ are superimposed

Fig. 7 Photographs of unfatigued and fatigued specimens (on the right in each pairing)

2.3 Flexural modulus

Some additional tests were performed to determine the flexural modulus and strength of polymer matrix composites, shown diagrammatically in Fig. 8. The flexural modulus is the ratio of the stress range and corresponding strain range. When calculating the flexural chord modulus, the recommended strain range is 0.002, with a start point of 0.001 and an end point of 0.003. The flexural modulus can be obtained from the stress-strain data for multidirectional or highly orthotropic composites using ASTM-D7264/D7264M and ASTM-D790.

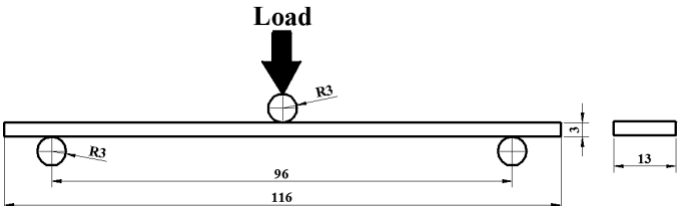

Fig. 8 Flexural modulus testing. Specimen dimensions and test setup for three-point loading experiments (according to ASTM-D7264/D7264M (2007)

Table 4 Mechanical properties of unfatigued composite specimens

Mechanical properties	Specimens			
	#800	#500	#300	#200
Flexural strength, S_0 (MPa)	354	375	348	312
Flexural modulus, E_0 (MPa)	18976	18452	17234	17823
Fatigue strength for 10^6cycles, S_N (MPa)	84.24	73.18	73.95	64.29
Hardness, H_0 (Barcol)	66.30	68.20	66.40	63.00

Table 5 The relationships among hardness, flexural strength and flexural modulus of unfatigued composite specimens

Specimens	The relationship between flexural strength and hardness	The relationship between flexural strength and hardness
#800	$S_0 = 5.33H_0$	$E_0 = 286H_0$
#500	$S_0 = 5.50H_0$	$E_0 = 271H_0$
#300	$S_0 = 5.24H_0$	$E_0 = 260H_0$
#200	$S_0 = 4.94H_0$	$E_0 = 283H_0$

$$\boldsymbol{E} = \frac{\Delta\sigma}{\Delta\varepsilon} \tag{4}$$

where $\boldsymbol{E}$ is the flexural modulus, $\Delta\sigma$ is the difference in flexural stress between the two selected strain points, and $\Delta\varepsilon$ is the difference between the two selected strain points (nominally 0.002).

The flexural moduli obtained for four different unfatigued (original) composite specimens are given in Table 4.

2.4 Hardness testing

Surface hardness testing was performed according to TS-EN-59 (1996) and ASTM-D2583 (2007) standards. The hardnesses of specimens were measured with a Barcol hardness tester (GYZ J934-1) (Muthukumar *et al*. 2011). The thickness of specimen should be no less than 1.5 mm, and any two indents should be within 3 mm of each other. Eight readings at each distance x = 3, 6, 9, 12, 15, 24, 30, 45, 60, 90, 120, and 190 mm from the fractured edge were taken for each specimen. The mean values are shown in Fig. 9, alongside the values of the flexural modulus at different

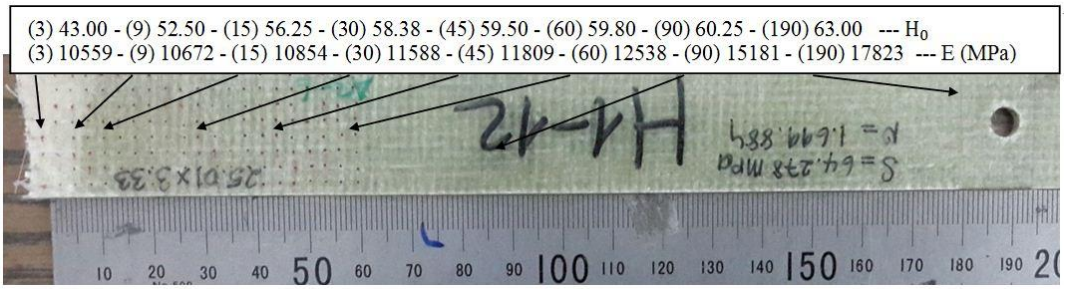

Fig. 9 *Degradation of hardness and modulus in fatigued GFRPs*. Average hardness and flexural modulus values for different distances from the fracture line (x = 3, 9, 15, 30, 45, 60, 90, and 190 mm)

distances from the fracture line for the group #200 specimen. Barcol hardness results for undamaged composite sheets similar to those used in this study are in (Becenen *et al*. 2010); the H values obtained were similar to this study above 50 Barcol. The hardness degradation have been calculated from Eq. (5) and are given in Table 6.

$$\boldsymbol{D_H} = 1 - H_x/H_0 \tag{5}$$

2.5 Stiffness testing

A simple test device, shown in Fig. 10, was used to measure the stiffness (flexural modulus). In this device, the stiffness values for the same distance were measured. Failed samples after about 1 million cycles (stage III) were loaded as cantilevers at a distance from the fracture point/free end (x = 3, 6, 9, 12, 15, 24, 30, 45, 60, and 90 mm). Keeping the moment distance stable (L = 100 mm), a load was applied from the free tip of the sample. Both the load (P) and deflection in the sample (δ) were recorded simultaneously. Moduli and other parameters were calculated using below equations

$$\sigma = \frac{6\,P\,L}{b\,h^2} \tag{6}$$

$$\delta = \frac{P\,L^3}{3\,E\,I} \tag{7}$$

$$E = \frac{P\,L^3}{3\,\delta\,I} \tag{8}$$

$$\varepsilon = \frac{\Delta\sigma}{\Delta E}\ (\text{Hooke}'\text{s Law}) \tag{9}$$

where b is the width of the beam, h is the thickness of the beam, σ is the stress at the outer surface, I is the moment of inertia, and ε is the maximum strain at the outer surface. For each load and deflection value, the modulus E was calculated from Eq. (8). In response to the applied regression (σ), from the basic Hooke's law given in Eq. (9), the shape change values (ε) were calculated. Thus, by using load-deflection data at hand, σ-ε curves were obtained. As explained in Section 2.3, by

using Eq. (4) (according to the ASTM-D7264/D7264M (2007)), real flexural moduli were calculated for each different distances. The flexural modulus degradations were calculated from Eq. (10). These values are given in Table 6.

$$\boldsymbol{D_E} = 1 - E_x/E_0 \tag{10}$$

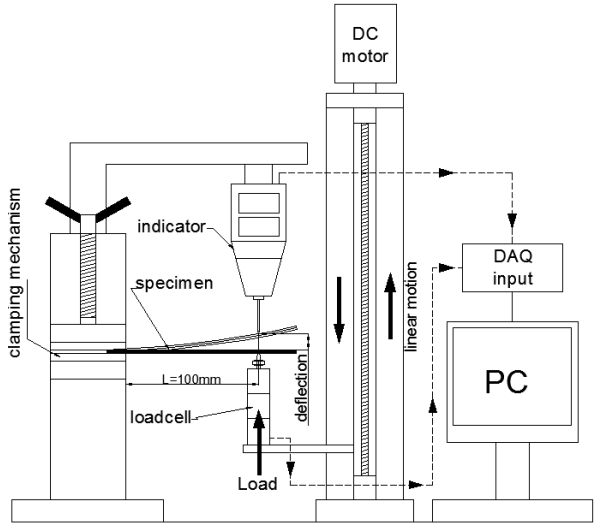

Fig. 10 Flexural stiffness testing of fatigued GFRPs. Cantilever-based test setup to determine stiffness degradation of the fatigued composite sheets

Table 6 The hardness and stiffness degradations of all samples in relation to distance from fracture line

x (mm) the distances from the fracture line	#800		#500		#300		#200	
	[a]H_0	E	H_0	E	H_0	E	H_0	E
3	49.00	11037	49.00	10845	49.75	10074	43.00	10559
6	52.13	11200	57.38	11000	53.13	10350	44.13	10600
9	54.00	11323	60.13	11191	56.63	10558	52.50	10672
12	55.75	11500	61.88	11820	59.13	10900	56.00	10750
15	56.50	11639	61.88	12464	59.38	11214	56.25	10854
24	61.25	11800	65.13	12680	60.88	11300	57.63	11250
30	62.13	12049	66.10	12910	61.70	11391	58.38	11588
45	62.63	12237	66.38	13828	61.75	11829	59.50	11809
60	63.60	13731	66.50	14297	62.13	12953	59.80	12538
90	63.75	14332	66.63	16375	62.75	13604	60.25	15181
120	65.00	not measured	67.40	not measured	64.60	not measured	61.60	not measured
190 (original)	66.30	18976	68.20	18452	66.40	17234	63.00	17823

[a] The data are the average values taken from a minimum of six test results

2.6 The hardness and stiffness degradation in fatigued samples

The total stiffness damage after about 1 million cycles in the stage III area of *S-N* curve are shown in Fig. 6. This means that the determination of the total losses of hardness and stiffness in the 3rd stage resulted in fracture of the specimen (cycling failure) and included the stiffness damage in the 1st and 2nd stages. For each composite sheet, the losses of hardness and stiffness were obtained as a function of the distance from the fractured edge and are given in Figs. 11(a) and (b). The relationship between hardness and stiffness degradations are shown in Fig. 11(c). A numerical comparison of the results is in Table 6.

3. Results and discussion

3.1 Comparison of the experimental data to the literature

The plots showing flexural moduli, hardnesses, and damage in the GFRP sheets are in Figs. 11(a)-(c). The maximum loss-values as a result of fatigue damage are given in Table 7. The relationship between hardness and stiffness degradation for all composite sheets are given in Fig. 11(c). Empirical formulae that relate to both hardness degradation and stiffness degradation for all sample groups are given in Table 8. For a fatigue limit of one million cycles in these composite sheets (before fracture), the hardness degradation corresponding to approximately 20% of flexural strength was seen to reach a minimum at 25% and stiffness degradation to reach a minimum at 41%.

Stiffness degradation in the samples at the end of testing in this study is higher than that in the literature. Here, the low-test frequency (0.5 Hz) is of great importance. At low frequency, stiffness degradation in composites may increase. In the study of Epaarachchi and Clausen (2003), it was found that, as long as the temperature of the sample does not change, as the loading frequency increases, the fatigue life of many polymer composite materials was extended as a result of the viscoelastic properties of the matrix material. That means a polymer composite material's stiffness degradation is inversely correlated with frequency and so is directly proportional to the fatigue life.

3.2 Macro and micro analysis

As seen in Fig. 12, the degree of whitening in the broken samples is very clear between x = 0 and x = 9 mm. Stress-whitening indicates the damaged area where the fibers were broken and the matrix is separated. Whitening between 0-9 mm in the upper layer indicates matrix damage and

Table 7 Maximum losses of hardness and stiffness of all samples in relation to 3-mm distance from the fracture line

Specimen	$D_H = 1 - (H_3/H_0)$	$D_E = 1 - (E_3/E_0)$
#800	0.26	0.42
#500	0.28	0.41
#300	0.25	0.42
#200	0.32	0.41

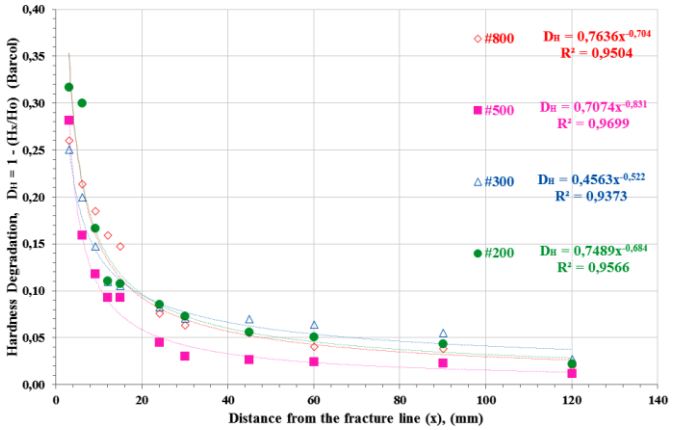

(a)

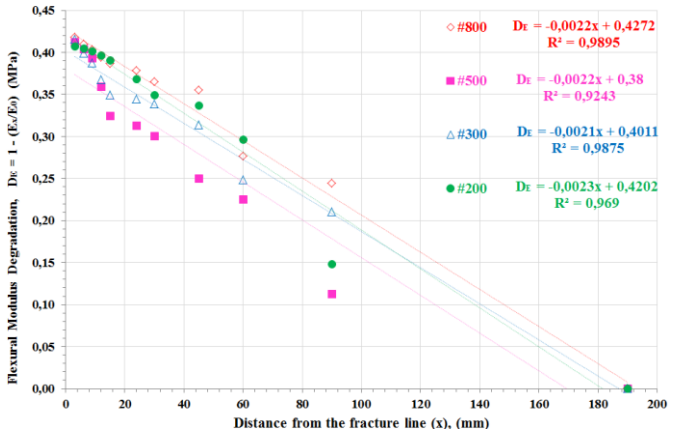

(b)

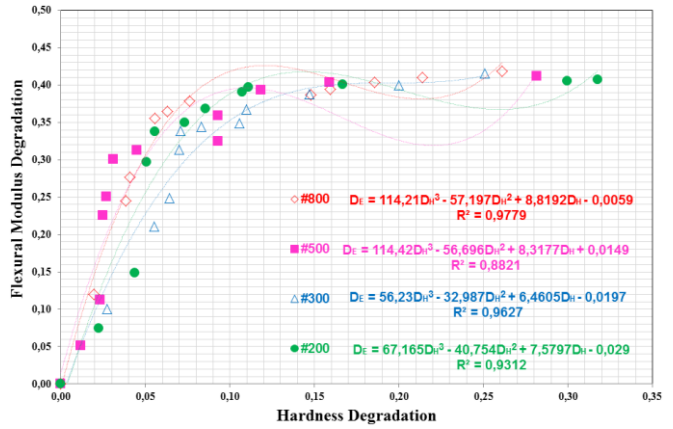

(c)

Fig. 11 *Damage in fatigued specimens*. The stiffness and hardness degradation graphs for glass-fiber composite sheets at various distances from the fracture line (x = 3, 6, 9, 12, 15, 24, 30, 45, 60, 90, and 120 mm): (a) hardness degradation; (b) stiffness degradation; and (c) the flexural modulus degradation versus the hardness degradation

Table 8 A comparison of stiffness degradation and damage criteria for 1 million cycles to the literature

Ref.	Loss of stiffness ratio	•Reinforcement •Fiber orientations	Related Eq. or Definition	•Matrix •Fiber-volume •Technique	•Fatigue test •Stress or strain-ratio (R) •Frequency or rpm •Test-control	Failure criteria
(Khan *et al.* 2001)	0.10	•Woven carbon fabric: ρ_w = 208 g/m^2 •(0,0,45,-45)	E = -3×10-6(N)+32.841	•Polyester •V_f = 66.6% •Prepreg fabric	•Tension-tension •R = 0.1 •Frequency = 20 Hz •Displacement-control	Modulus degradation rate (dE/dN)
	0.15	•Woven carbon fabric: ρ_w = 208 g/m^2 •(45,-45,0,0)	E = -1.1×10^{-6}(N)+33.522			
(Poursarti and Beaumont 1983)	0.35	•Carbon fiber	$E = 0.65E_0$	•Epoxy resin •(45/90/-45/0)$_S$ •Hand lay-up	•R = 0.1	When delamination and matrix cracking are complete, $E = 0.65E_0$
(Selmy *et al.* 2013)	0.19	•Rovingfiber-glass: ρ_L = 2.4 g/m •Unidirectional (U_5)	Residual stiffness ratio $(EI)/(EI)_0 = 1.37(N)^{-0.038}$	•Epoxy resin •V_f = 37.0% •Hand y-up	•Cantilever plane-bending •R = -1 •Frequency = 23.6 Hz •Deflection-control	20% reduction of the initial flexural stiffness was taken as a failure criterion.
	0.21	•Random fiber glass: ρ_w = 900 g/m^2 Chopped randomly oriented mat random glass (R_5)	Residual stiffness ratio $(EI)/(EI)_0 = 1.50(N)^{-0.046}$			
(Abd-Allah *et al.* 1997)	0.30	•Roving fiber-glass: ρ_L = 1150 g/km •Unidirectional	The endurance limit (S_e) of the test specimen was defined as the upper limit value of stress at which the residual stiffness ratio $(EI)/(EI)_0$ of the test specimen is ≥ 0.7	•Polyester •V_f = 44.7% •Pultrusion	•Rotating flexural •R = -1 •Frequency = 25 Hz •Load-control	The failure criterion was defined as when residual stiffness of the test specimen reached 70% of the specimen stiffness at the start of the test (ASTM-D671 1993)
(Keller *et al.* 2005)	0.59	•Roving fiber-glass •Random fiber glass: ρ_w = 300 g/m^2 Chopped randomly oriented mat	$E = 0.41E_0$	•Polyester •V_f = 46-47% •Pultrusion	•Tension-tension •R = 0.1 •Frequency = 12 Hz •Load-control	A loss of specimen stiffness up to 50% during the fatigue experiments was observed and can only be explained by considerable fiber failures.
Present study	0.26^{D_H} 0.42^{D_E}	#800	$(H = 0.74H_0)$ $(E = 0.58E_0)$	•Polyester •V_f = 44% •RTM	•Cantilever plane-bending •R = -1 •Frequency = 0.5 Hz •Load-control	25% reduction of the initial hardness and 41% reduction of the initial flexural modulus were taken as a failure criteria
	0.28 0.41	#500	$(H = 0.72H_0)$ $(E = 0.59E_0)$			
	0.25 0.42	#300	$(H = 0.75H_0)$ $(E = 0.58E_0)$			
	0.32 0.41	#200	$(H = 0.68H_0)$ $(E = 0.59E_0)$			

D_H: Hardness degradation; D_E: Flexural modulus degradation

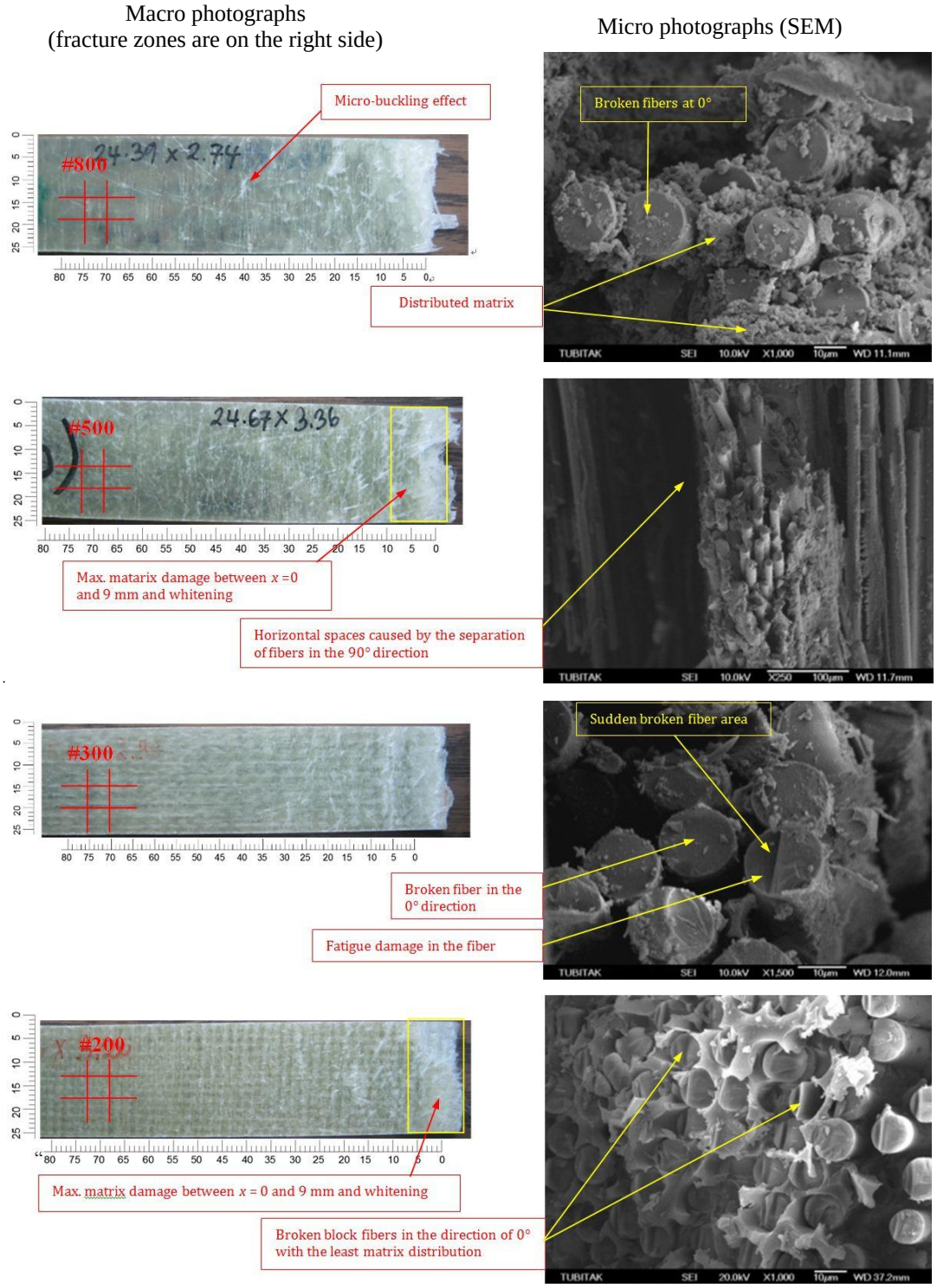

Fig. 12 *Failure analysis*. Macrographs (optical) and micrographs (SEM) of the failure surfaces and their explanations

fiber breakage at the macroscale. Farther from fracture line, the white areas decrease in size. Other sources of whitening near the upper surface is the result of micro-cracking between fibers and the matrix (Mayer 1996). After fatigue fracture, optical (macro) photographs of the composite specimens, especially those at stage III (one million cycles) were taken and a scanning electron microscope analysis was performed (Davies and Petton 1999, Bezazi *et al*. 2003, El-Wafa 2004). The nature of the fracture zone, the origin of the whitening, and the damage to the interior structure are given with explanations in Fig. 12.

3.3 Decrease in the stiffness

Because the composite samples in the current study were subjected to fully reversed loading, the maximum tensile and compressive stresses occur on the upper and lower surfaces the specimen, respectively. These stresses during fatigue testing cause micro-buckling in fibers at crossing points (Fig. 12(a)) of woven-roving fabric bundles (Caprino and Giorleo 1999). On a local scale, micro-buckling of the fibers can occur due to misalignment of the 0 degree reinforcement or small voids in the resin (Mayer 1996). Because of these micro-bucklings, areal whitening develops and the stiffness decreases, even there is no fracture in the specimen (Fig. 12).

4. Conclusions

This paper includes experimental and analytical studies to the relationship between Barcol hardness and flexural modulus degradation of composite sheets after flexural fatigue. From the experimental and analytical studies, conclusions can be summarized as follows.

- Hardness of composite sheets is directly related to the flexural modulus. This situation is also true for the composites working under dynamic loading.
- There is a reasonably well-defined relationship between Barcol hardness and flexural modulus degradation in the distance range studied.
- The hardness and stiffness degradation were determined in the region closest to the fracture line (< 3 mm distant); hardness degradation was 0.25 (min. #300) and 0.32 (max. #200), stiffness degradation was 0.41 (min. #500 and #200) and 0.42 (max. #800 and #300).
- Considering the maximum and minimum losses for all specimen groups, a 25% reduction of the initial hardness and 41% reduction of the initial flexural modulus can be taken as the failure criteria.
- The critical distance for hardness loss is 30 mm. While the hardness drops of quickly up to 30 mm, hardness degradation greatly slowed down at distances > 30 mm. The original, base hardness values were attained after 150 mm. For the flexural modulus, this critical value was 9 mm, i.e., the flexural modulus quickly dropped until 9 mm, after which the decline slowed. Unlike the trend in the hardness, stiffness degradation was observed up to the loading point (190 mm).
- Hardness degradation was reduced to 5% in the range 35-60 mm from the fracture edge. However, a lost stiffness of 5% was only attained after 150 mm; stiffness degradation for same distance from the fracture edge is much more than hardness degradation.
- Other researchers evaluated the elastic modulus change and used stiffness degradation as

the primary damage criterion. This study also has shown that, along with stiffness degradation, there is a hardness degradation that can also be considered to be a damage criterion for GFRP composite parts, such as those in wind turbine blades.

- Surface hardness values to be taken at critical areas of dynamic components, such as those in wind turbines, give information about the extent of damage, and deviations at the cycling orbit of the blade tip point give information about stiffness degradation. When the assessment procedures are performed on these components after specific intervals, the results should be compared to these critical values. When any critical assessment is reached, it should be understood that composite structure has completed its life term.

Acknowledgments

This study has been partly granted by the Unit of Scientific Research Projects in Balıkesir University. Besides, the authors would like to thank Poliya Company, Fibroteks Woven Company and Glass-Fiber Company (Şişecam) for their material and workmanship support.

References

Abd-Allah, M.H., Abdint, E.M., Selmy, A.I. and Khashaba, U.A. (1997), "Effect of mean stress on fatigue behaviour of GFRP pultruded rod composites", *Compos. Part A*, **28A**(1), 87-91.

ASTM-D671 (1993), Flexural Fatigue of Plastics by Constant-Amplitude-of-Force.

ASTM-D2583 (2007), Indentation Hardness of Rigid Plastics by Means of a Barcol Impressor, American Society for Testing and Materials.

ASTM-D790 (2010), Standard Test Methods for Flexural Properties of Unreinforced and Reinforced Plastics and Electrical Insulating Materials, American Society for Testing and Materials.

ASTM-D7264/D7264M (2007), Standard Test Method for Flexural Properties of Polymer Matrix Composite Materials, American Society for Testing and Materials.

ASTM-D3039/D3039M (2008), Standard Test Method for Tensile Properties of Polymer Matrix Composite Materials, American Society for Testing and Materials.

Ay, İ., Sakin, R. and Okoldan, G. (2008), "An improved design of apparatus for multi-specimen bending fatigue and fatigue behaviour for laminated composites", *Mater. Des.*, **29**(2), 397-402.

Bao, Y.W., Wang, W. and Zhou, Y.C. (2004), "Investigation of the relationship between elastic modulus and hardness based on depth-sensing indentation measurements", *Acta Mater.*, **52**(18), 5397-5404.

Becenen, N., Eker, B. and Sahin, M. (2010), "Mechanical properties of plastic matrix composite materials used in tractor bonnets", *J. Reinf. Plast. Compos.*, **29**(24), 3637-3644.

Belingardi, G. and Cavatorta, M. (2006), "Bending fatigue stiffness and strength degradation in carbon–glass/epoxy hybrid laminates: Cross-ply vs. angle-ply specimens", *Int. J. Fatigue*, **28**(8), 815-825.

Belingardi, G., Cavatorta, M.P. and Frasca, C. (2006), "Bending fatigue behavior of glass–carbon/epoxy hybrid composites", *Compos. Sci. Technol.*, **66**(2), 222-232.

Bezazi, A.R., Mahi, A.E., Berthelot, J.-M. and Bezzazi, B. (2003), "Flexural Fatigue Behavior of Cross-Ply Laminates: An Experimental Approach", *Strength Mater.*, **35**(2), 149-161.

Bezazi, A., Pierce, S., Worden, K. and Harkati, E. (2007), "Fatigue life prediction of sandwich composite materials under flexural tests using a Bayesian trained artificial neural network", *Int. J. Fatigue*, **29**(4), 738-747.

Caprino, G. and Giorleo, G. (1999), "Fatigue lifetime of glass fabric/epoxy composites", *Compos. Part A*, **30**, 299-304.

Davies, P. and Petton, D. (1999), "An experimental study of scale effects in marine composites", *Compos.*

Part A, **30**(3), 267-275.
El Mahi, A., Khawar Farooq, M., Sahraoui, S. and Bezazi, A. (2004), "Modelling the flexural behaviour of sandwich composite materials under cyclic fatigue", *Mater. Des.*, **25**(3), 199-208.
El-Wafa, M.A.E.-W.M. (2004), *Fatigue Behavior of Notched Gfr/Epoxy Composites*, M.Sc. Dissertation; Zagazig University, Zagazig, Egypt.
Epaarachchi, J.A. and Clausen, P.D. (2003), "An empirical model for fatigue behavior prediction of glass fibre-reinforced plastic composites for various stress ratios and test frequencies", *Compos. Part A*, **34**(4), 313-326.
Goeij, W.C.d., van Tooren, M.J.L. and Beukers, A. (1999), "Implementation of bending-torsion coupling in the design of a wind-turbine rotor-blade", *Appl. Energy*, **63**(3), 191-207.
Jha, K.N. (2012), *Development of a Small Wind Power Generation Facility*, M.Sc. Dissertation; Jadavpur University, Kolkata, India.
Kar, N.K., Barjasteh, E., Hu, Y. and Nutt, S.R. (2011), "Bending fatigue of hybrid composite rods", *Compos. Part A*, **42**(3), 328-336.
Keller, T., Tirelli, T. and Zhou, A. (2005), "Tensile fatigue performance of pultruded glass fiber reinforced polymer profiles", *Compos. Struct.*, **68**(2), 235-245.
Kensche, C. (2006), "Fatigue of composites for wind turbines", *Int. J. Fatigue*, **28**(10), 1363-1374.
Khan, Z., Al-Sulaiman, F.A., Farooqi, J.K. and Younas, M. (2001), "Fatigue life predictions in woven carbon fabric/polyester composites based on modulus degradation", *J. Reinf. Plast. Compos.*, **20**(5), 377-398.
Koricho, E.G., Belingardi, G. and Beyene, A.T. (2014), "Bending fatigue behavior of twill fabric E-glass/epoxy composite", *Compos. Struct.*, **111**, 169-178.
Kumar, S., Roy, N. and Ganguli, R. (2007), "Monitoring low cycle fatigue damage in turbine blade using vibration characteristics", *Mech. Syst. Sig. Process.*, **21**(1), 480-501.
Mayer, R.M. (1996), *Design of Composite Structures Against Fatigue*, Design of Composite Structures Against Fatigue, Great Britain, Antony Rowe Ltd., Effects of Environment, pp. 72-73.
Meththananda, I.M., Parker, S., Patel, M.P. and Braden, M. (2009), "The relationship between Shore hardness of elastomeric dental materials and Young's modulus", *Dent. Mater.*, **25**(8), 956-959.
Muthukumar, T., Aravinthan, A., Lakshmi, K., Venkatesan, R., Vedaprakash, L. and Doble, M. (2011), "Fouling and stability of polymers and composites in marine environment", *Int. Biodeterior. Biodegrad.*, **65**(2), 276-284.
Natarajan, V. (2005), "Fatigue response of fabric-reinforced polymeric composites", *J. Compos. Mater.*, **39**(17), 1541-1559.
Paepegem, W.V. and Degrieck, J. (2002), "A new coupled approach of residual stiffness and strength for fatigue of fibre-reinforced composites", *Int. J. Fatigue*, **24**(7), 747-762.
Philippidis, T.P. and Vassilopoulos, A.P. (1999), "Fatigue of composite laminates under off-axis loading", *Int. J. Fatigue*, **21**(3), 253-262.
Poursartip, A. and Beaumont, P.W.R. (1983), *A Damage Approach to the Fatigue of Composites*, In: (Z. Hashin and C.T. Herakovich Eds.), *Mechanics of Composite Materials*: *Recent Advances*, Elsevier Inc., pp. 449-456, UK.
Sakin, R. and Ay, İ. (2008), "Statistical analysis of bending fatigue life data using Weibull distribution in glass-fiber reinforced polyester composites", *Mater. Des.*, **29**(6), 1170-1181.
Sakin, R., Ay, İ. and Yaman, R. (2008), "An investigation of bending fatigue behavior for glass-fiber reinforced polyester composite materials", *Mater. Des.*, **29**(1), 212-217.
Selmy, A. I., Azab, N.A. and Abd El-baky, M.A. (2013), "Flexural fatigue characteristics of two different types of glass fiber/epoxy polymeric composite laminates with statistical analysis", *Compos. Part B*, **45**(1), 518-527.
TS-EN-59 (1996), *Glass Fiber Reinforced Plastics - The Measurement of Hardness with Barcol Hardness Device* (*934-1*), TS-EN-59, Turkish Standards Institute (TSE), Ankara, Turkey.
Vavouliotis, A., Paipetis, A. and Kostopoulos, V. (2011), "On the fatigue life prediction of CFRP laminates using the Electrical Resistance Change method", *Compos. Sci. Technol.*, **71**(5), 630-642.

Xu, H.H.K., Smith, D.T., Schumacher, G.E., Eichmiller, F.C. and Antonucci, J.M. (2000), "Indentation modulus and hardness of whisker-reinforced heat-cured dental resin composites", *Dent. Mater.*, **16**(4), 248-254.

CC

Nomenclature

E	flexural modulus	b	width of beam (mm)
E_0	flexural modulus for unfatigued specimen	h	thickness of beam (mm)
EI	the flexural stiffness	σ	stress at the outer surface
P	the applied load	δ	deflection (mm)
L	the cantilever length	ε	maximum strain at the outer surface
I	moment of inertia	H	Barcol hardness (HBa)
N_f	the number of cycles to failure	x	the distance from the fracture line
V_f	fiber volume fraction	D_H	hardness degradation
ρ	density	D_E	flexural modulus degradation
R	loading rate	H_0	Barcol hardness for unfatigued specimen
S_f	stress amplitude	S_0	flexural strength for unfatigued specimen
m and n	constants	S_N	fatigue strength for 10^6 cycles